Morphology, Thermal Expansion, and Electrical Conductivity of Multiwalled Carbon Nanotube/Epoxy Composites

Alexandre S. dos Santos,[1] Thiago de O. N. Leite,[2] Clascídia A. Furtado,[2] Cezar Welter,[1] Luiz C. Pardini,[3] Glaura G. Silva[1]

[1]*Departamento de Química/Universidade Federal de Minas Gerais, Caixa Postal 702, 31270-901, Belo Horizonte, MG, Brazil*
[2]*Centro de Desenvolvimento da Tecnologia Nuclear/Comissão Nacional de Energia Nuclear, Belo Horizonte, MG, Brazil*
[3]*Centro Técnico da Aeronáutica/IAE, São José dos Campos, SP, Brazil*

Received 16 April 2007; accepted 22 October 2007
DOI 10.1002/app.27614
Published online 18 January 2008 in Wiley InterScience (www.interscience.wiley.com).

ABSTRACT: Multiwalled carbon nanotube/epoxy composites loaded with up to 0.5 wt % multiwalled carbon nanotubes were prepared and characterized. Infrared microscopy, scanning electron microscopy, thermogravimetry, differential scanning calorimetry, thermomechanical analysis, and electrical conductivity measurements of the composites were performed. Infrared microscopy and scanning electron microscopy images showed that the debundled nanotubes were well dispersed. The thermal expansion coefficients, before and after the glass transition, remained approximately constant with the addition of nanotubes, whereas the electrical conductivity at room temperature increased approximately 5 orders of magnitude. This result was attributed to the thermal expansion coefficients of the intertube gap on the carbon nanotube bundles, which were in the same range as that of the epoxy resin. Therefore, nanocomposites capable of electrostatic dissipation can be processed as neat epoxy materials with respect to the volume changes with temperature. © 2008 Wiley Periodicals, Inc. J Appl Polym Sci 108: 979–986, 2008

Key words: composites; morphology; nanocomposites; thermal properties

INTRODUCTION

Single-walled carbon nanotubes (SWNTs) and multiwalled carbon nanotubes (MWNTs)[1] present remarkable mechanical properties as carbon nanotubes (CNTs) can relax elastically when stress is released, whereas carbon fibers fracture easily under compression.[2] A low CNT composite loading can be used to obtain high-performance levels suitable for specific applications in comparison with those of conventional fillers such as carbon black.[3] Although the CNT production cost is higher than that of conventional fillers, its low loading is advantageous because the effects on resin properties are minimal and the same processing equipment can be used with neat resins and nanocomposites. However, it has been frequently emphasized that the use of CNTs as structural reinforcements, specifically of polymer composites, depends on the ability to transfer the load from the matrix to the nanotubes.[4] Two factors are most critical for load transfer: (1) a homogeneous nanotube dispersion through the matrix and (2) strong CNT–polymer interfacial bonding.

Epoxy-based composites are materials of high technological interest because of features such as their mechanical and thermal properties. A large number of recent works have dealt with CNT-reinforced epoxy (e.g., refs. 3 and 5–17). Different processes and controversial results were reported earlier concerning the improvement of their mechanical and thermal properties. However, recent works,[3,17] which show good CNT dispersion and improvements in interfacial adhesion by nanotube functionalization, have indicated significant enhancement of mechanical properties with low CNT loadings. Furthermore, there is agreement on the fact that these composites show a low percolation threshold (<0.5 wt %) and an increase of more than 6 orders of magnitude in electrical conductivity, reaching values close to 10^{-2} S/m.[12–15]

The thermal expansion coefficient of SWNT bundles has been determined by X-ray diffraction studies.[18] Three values have been obtained for the temperature range from 300 to 950 K: $(-0.15 \pm 0.20) \times 10^{-5}$ K^{-1} for the tube diameter, $(0.75 \pm 0.25) \times 10^{-5}$ K^{-1} for the triangular lattice, and $(4.2 \pm 1.4) \times 10^{-5}$

Correspondence to: G. G. Silva (glaura@qui.ufmg.br).
Contract grant sponsor: Agência Espacial Brasileira (Programa Uniespaço).
Contract grant sponsor: Instituto do Milênio de Nanociências/Programa de Apoio ao Desenvolvimento Cientifico e Tecnológica/Conselho Nacional de Pesquisa/Ministério de Ciência e.

K^{-1} for the intertube gap. The tube-diameter thermal expansion coefficient value is negligible on account of the accuracy, which is consistent with the seamless tube structure formed by strong covalent bonds between carbon atoms, as pointed out by Maniwa et al.[18] On the other hand, the intertube gap value is larger than the thermal expansion coefficient in the *c* axis of graphite (2.6×10^{-5} K^{-1}), which is important for analyzing the behavior of SWNT composites in comparison with other carbon-based composites. Maniwa et al.[19] also investigated the thermal expansion coefficient of MWNTs. They reported a widely distributed range of 1.6×10^{-5} to 2.6×10^{-5} K^{-1}. This distribution was associated with the presence of a well-defined concentric tubule structure and highly defective MWNTs.

Wei et al.[20] reported a thermal expansion study of CNT–polyethylene composites by molecular dynamics simulation. These authors predicted an increase in the thermal expansion of a composite material with the addition of nanotubes. This behavior was not observed in experimental works[21,22] with different polymers. Guo et al.[21] investigated polyacrylonitrile, and Xu et al.[22] studied poly(vinylidene fluoride); both used high SWNT concentrations, 40 wt % and up to 49 vol %, respectively. These works used thermomechanical analysis (TMA) to determine the thermal expansion coefficient and reported a decrease in this parameter for composites in relation to those of the pure polymers. Yuen et al.[16] presented results of the thermal expansion coefficient before the glass transition for an MWNT/epoxy system. These authors observed a decrease for the neat epoxy from 6.23×10^{-5} to 5.98×10^{-5} $°C^{-1}$ for a 10 wt % MWNT composite. Furthermore, Wang et al.[23] also reported the thermal expansion coefficient for an epoxy system composite with pristine and functionalized SWNTs. The SWNT loading was 1 wt % in all composites, and an approximately 50% reduction in the thermal expansion coefficient of the composites was observed below the glass transition. On the other hand, the composite thermal expansion coefficients increased over the glass transition in relation to those of the neat epoxy.

A preliminary nanotube network disentanglement procedure was applied in this work to improve the MWNT dispersion in the epoxy resin. Morphological, thermomechanical, and direct-current conductivity properties of the nanotube-based composites were investigated in a low nanofiller concentration range. This range was selected because recent works pointed to significant changes in electrical, mechanical, and thermal properties with filler contents up to 0.5 wt %.[3,9,10,13–15,17] Moreover, a low loading range allows better dispersion and makes composite processing easier. Although extensive studies have reported on the conductivity of nanotube–epoxy composites, the thermal expansion behavior, an important material property for many applications, is still largely unexplored.

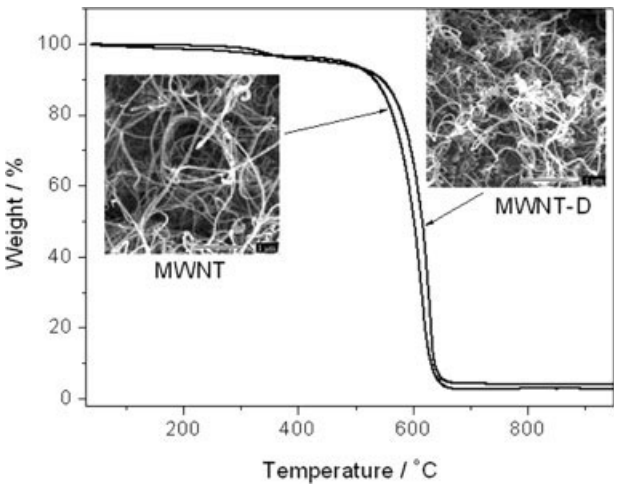

Figure 1 TG curves of MWNT and MWNT-D (treated for bundle dispersion) and representative MWNT SEM images before and after debundling.

EXPERIMENTAL

Materials

An MWNT material synthesized by chemical vapor deposition (CNT Co., Incheon, Korea) was employed in this work. The ranges of the nanotube diameter and length given by the supplier were 10–40 nm and 5–20 μm, respectively. Scanning electron microscopy (SEM) analysis (model JSM-6360 LV, JEOL) showed an open structure consisting of entangled bundles with diameters between 50 and 200 nm (Fig. 1). The Brunauer–Emmett–Teller specific surface area, measured by nitrogen adsorption (NOVA 2200, Quantachrome Co.), was 136 m^2/g, and the mesoporous volume was 0.4 cm^3/g. These values are characteristic of an open mesoporous network of entangled bundles,[24] which is in agreement with SEM observations. The MWNT material presented a fraction of residual metal of approximately 2.8 wt % (calculated as $\sim$70% of the final residue weight and corresponding to Ni, Co, or Fe metallic oxides), as shown by the thermogravimetric residue of $\sim$ 4 wt % in Figure 1.

The epoxy resin, XR1555, was commercially available and was used with HY-951 Aradur hardener; both were supplied by Vantico, Inc. (London, UK) The viscosity of the epoxy resin based on diglycidyl bisphenol A (DGEBA) was between 4 and 6 Pa s at 25°C, and the density was between 1.15 and 1.20 g/cm^3 at 20°C. The hardener was an aliphatic amine (triethanolamine).

Preliminary debundling procedure

MWNTs were suspended in a 1 wt % aqueous sodium dodecyl sulfate (SDS) solution according to the procedure described by Connell et al.[25] Briefly, 1 wt % surfactant was combined with 100 mg of the nanotube material in 1000 mL of water, and the mixture was ultrasonicated in the bath at a power level of 40 W for 90 min. The suspension was centrifuged for 30 min at 6000 rpm to separate impurities and large bundles. Acetone was then added to the supernatant to flocculate and remove nanotubes from the suspension. The disentangled nanotube material (MWNT-D) was filtered through a Millipore polytetrafluoroethylene membrane (Billerica, MA) filter with a pore diameter of 1.2 μm and carefully washed with methanol to remove the surfactant. The characteristics of the debundled MWNT-D are presented in the Results and Discussion section.

Preparation of the MWNT/epoxy nanocomposites

Two series of composites were prepared for comparison: MWNT/epoxy (series 1) and MWNT-D/epoxy (series 2). The raw nanotubes were dispersed in the epoxy resin with simultaneous low mechanical stirring and strong sonication for series 1. Next, the hardener was added to the nanotube/epoxy mixture, and the complete formulations were also subjected to low mechanical agitation with strong sonication. The procedure to prepare series 1 is distinct from that of series 2 because of the use of a solvent (acetone) to disperse MWNT-D before its introduction into the epoxy resin in the latter. Thus, series 2 composites had the advantage of the narrower bundle dimension of MWNT-D and the solvent dispersion of the nanotubes in the epoxy resin. After the dispersion of MWNT-D in epoxy, the mixture was maintained in a vacuum oven at 60°C for 15 h for solvent evaporation, and in sequence, the hardener was added with low mechanical agitation and strong sonication.

Finally, the samples were placed in a mold with 50 mm in diameter and 2 mm thick, and both series were cured with strictly the same procedure: (1) they were subjected to a temperature ramp of 1°C/min up to 40°C and kept isothermal for 2 h at 40°C and (2) they were subjected to a temperature ramp of 1°C/min up to 60°C and kept isothermal for 8 h at 60°C. The reaction was completed in a vacuum stove for 7 days at 30°C. A low concentration range of the filler (up to 0.5 wt %) was studied. Therefore, the main goal was to compare the effects of this load range on the conductivity and thermal expansion simultaneously.

Characterization of the MWNT/epoxy nanocomposites

A laboratory-made infrared microscopy setup was used to visualize the degree of MWNT dispersion in the nanocomposite systems. The nanocomposite morphology was characterized with SEM (model JSM-6360 LV, JEOL) with a 7.5-nm gold covering produced by 30-s metallization, an acceleration tension of 25 kV, and a sample current of 6.0×10^{-11} A.

For electrical conductivity measurements, 1-mm-thick samples were cut with a 0.7-cm^2 surface and polished. Opposing sides were painted with conductive silver paint to control the contact area during measurement. The direct-current electrical conductivity of the bulk was determined in triplicate by the measurement of the electrical current through the sample when a potential of 50 V was applied. Data were collected with a Keithley 238 high-current measuring unit.

Thermomechanical properties were investigated with a TMA 2940 thermomechanical analyzer (TA Instruments, New Castle, DE) in the expansion mode with a force of 0.05 N. The samples were heated from −50 to 250°C at 5°C/min in an N_2 atmosphere at 100 mL/min. The thermal study was performed with a DSC 2920 modulated differential scanning calorimetry (DSC) apparatus (TA Instruments) with samples of approximately 10 mg heated from −100 to 200°C at a scan rate of 10°C/min in a helium atmosphere at 40 mL/min. Thermogravimetry (TG) measurements were performed in an SDT 2960 thermogravimetry/dynamic thermal analysis (TG–DTA) apparatus (TA Instruments). Samples of approximately 10 mg were heated from 25 to 800°C at a scan rate of 10°C/min in an air atmosphere at 100 mL/min in TG–DTA runs. The data obtained from TG, DSC, and TMA measurements were determined at least in duplicate.

RESULTS AND DISCUSSION

Figure 1 shows TG curves and SEM images illustrating the MWNT characteristics before and after the preliminary debundling procedure. The images are on the same scale and are representative of the whole sample. By comparing the two images, we can notice that the nanotube bundles seem to be narrower after sonication in an aqueous SDS solution (MWNT-D) and are now shorter. The diameter of 20 bundles was evaluated from several images in different regions of both samples. An average decrease of ~30% in the bundle diameter after processing was observed.

Because the epoxy resin is transparent to infrared light, the benefits of the previous debundling process and solvent dispersion in getting homogeneous CNT–epoxy nanocomposites could be evaluated with infrared optical microscopy transmission images. Figure 2 compares infrared microscopy images of 0.25 wt % nanotube composites of series 1 and 2. Similar patterns were observed for the other

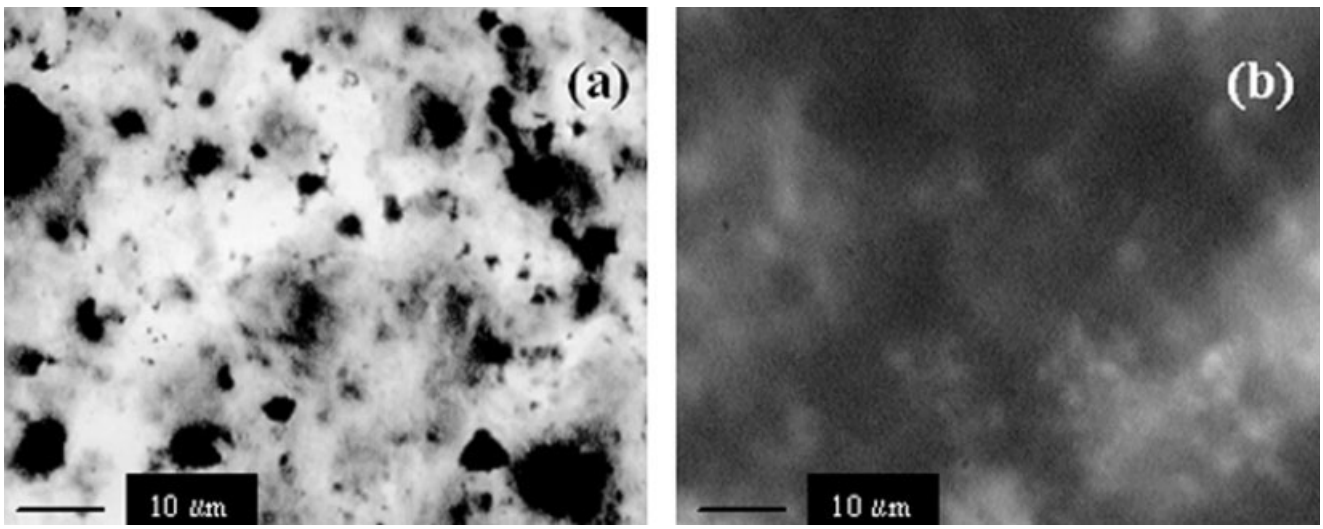

Figure 2 Infrared optical microscopy images (100×) for (a) the 0.25 wt % MWNT/epoxy composite (series 1) and (b) the 0.25 wt % MWNT-D/epoxy composite (series 2).

compositions in both series. A heterogeneous composite material with micrometric MWNT bundle aggregates clearly identified in the transparent resin was obtained without solvent dispersion. The MWNT-D dispersion of series 2 composite samples was significantly improved. Figure 2(b) exhibits a much more homogeneous composite material. Several groups (e.g., refs. 9, 10, 12, 15, and 16) previously reported the successful enhancement of a dispersion by using a solvent, especially acetone, in the preparation of CNT in epoxy composites, and so is the case in this work.

Morphological characterization

SEM images of fracture surfaces were used to examine the morphology of the neat resin and nanocomposites in detail. As can be observed in Figure 3, the morphology of the composite samples of both series 1 [MWNT/epoxy systems; Fig. 3(b)] and series 2 [MWNT-D/epoxy systems; Fig. 3(d)] is considerably changed in comparison with the respective neat epoxy resins [Fig. 3(a,c)]. The unidirectional cleavage and smooth fracture surfaces of the neat epoxy matrices became isotropic and rough after the introduction of the fillers. A similar behavior was observed by Liao et al.[9] for epoxy samples containing 0.5 wt% SWNT dispersed with a surfactant and acetone.

High-magnification SEM images of the epoxy and composite fracture surfaces are illustrated in Figure 4. They show areas in the composite samples containing nanotubes. In the low concentration range considered in this work, the nanotubes seem to be well impregnated by the epoxy matrix, and aggregates are under 100 nm. No micrometric aggregates are observable in these images. However, the MWNT aggregates (series 1) are concentrated in small areas, as shown in the composite fracture surface [Figs. 3(b) and 4(b), rounded by a circle], whereas in MWNT-D-based composites (series 2), the nanotube bundle distribution seems more homogeneous throughout the entire surface [Figs. 3(d) and 4(d,e)].

The SEM images also indicate the good efficiency of the solvent dispersion of MWNTs in the epoxy matrix. Therefore, from now on, only the results obtained for series 2 nanocomposites will be fully presented for the sake of conciseness. When the comparison of the properties of the two series of composites is interesting, the results obtained for series 1 will be mentioned.

Electrical conductivity

The results for the room-temperature electrical conductivity of series 2 materials are shown in Table I. The value obtained for the pure epoxy is in good agreement with those of other works, which reported conductivities from 10^{-14} to 10^{-12} S/m for neat epoxy materials.[12,13] The percolation threshold can be defined as the filler content for conductivity $\geq 10^{-6}$ S/m,[14] and for CNT/epoxy systems, some authors[13–15] have reported this critical value to be less than 0.1 wt %, as mentioned earlier in this report. On the other hand, percolation thresholds of 0.3 and 0.6 wt % were obtained by Barrau et al.[12] and Yuen et al.,[16] respectively. These discrepancies are probably associated with different raw materials (the epoxy resin and hardener), different CNT characteristics, and distinct composite preparation methodologies. The conductivity value obtained for the 0.5 wt % MWNT-D composite in this work (Table I) indicates that this concentration is close to the critical mass value.

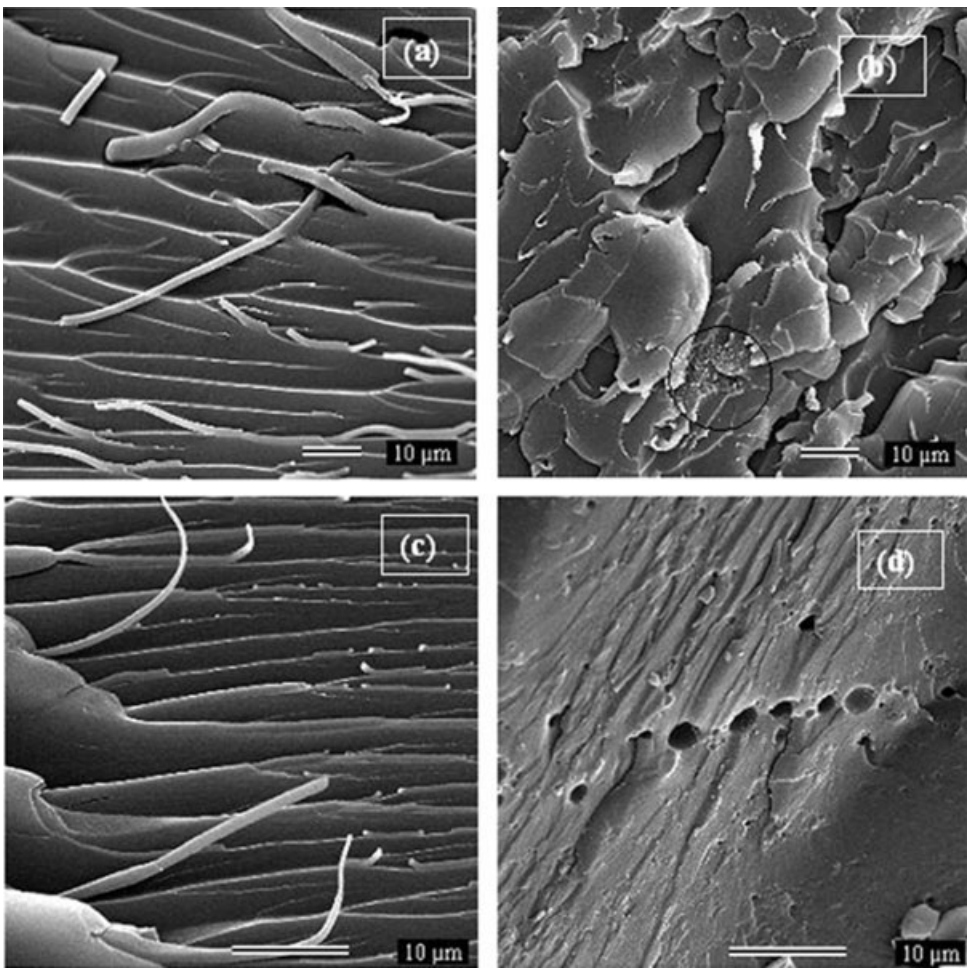

Figure 3 SEM images of fracture surfaces of (a) the neat epoxy resin, (b) the 0.1 wt % MWNT/epoxy composite (series 1), (c) the neat epoxy resin prepared with a solvent (acetone), and (d) the 0.5 wt % MWNT-D/epoxy composite (series 2).

Thermal analysis

The existence of either residual surfactant or solvent in the MWNT-D material was checked by TG. Figure 1 shows the TG curves of the MWNT sample before and after debundling in air at 10°C/min. The curves are very similar; both exhibit one prominent weight loss with a corresponding sharp TG peak derivative at ~ 620°C. A small weight loss can be observed at 315°C, and it increases from 2% for MWNT to ~ 5% for MWNT-D; a residue increase from 2.7 to 3.8% occurs after debundling. Despite the exhaustive washing, there was some residual material in the MWNT-D sample. However, this residual material had no significant influence on the CNT thermal stability.

All composites (series 1 and 2) investigated in this work showed similar TG curves in air (not shown), with two decomposition steps characterized by maximum decomposition rates at 350 and 530°C. No noticeable weight loss occurred below 100°C for MWNT-D-based composites prepared with acetone, and this was ascribed to the high volatility of the solvent.

The thermal stability of series 2 composites (prepared with MWNT-D/acetone) decreased slightly as a function of the nanotube concentration, whereas no significant change was observed for that of series 1. For instance, no series 1 materials presented weight loss at 200°C. The values for series 2 are displayed in Table I. The increase in the weight-loss values of MWNT-D/epoxy composites at 200°C indicates a more defective structure of the MWNT-D composites in comparison with the MWNT/epoxy system results. This could be a result of the residual presence of the surfactant in MWNT-D, even if we consider the very low content of the filler in the composite. Another possibility is that the introduction of nanotubes into the epoxy resin in the presence of acetone may have induced a more defective polymer structure after cure.

Figure 5 shows DSC curves for materials of series 2. The glass-transition temperatures (T_g's) of all samples were determined as the peak temperatures in

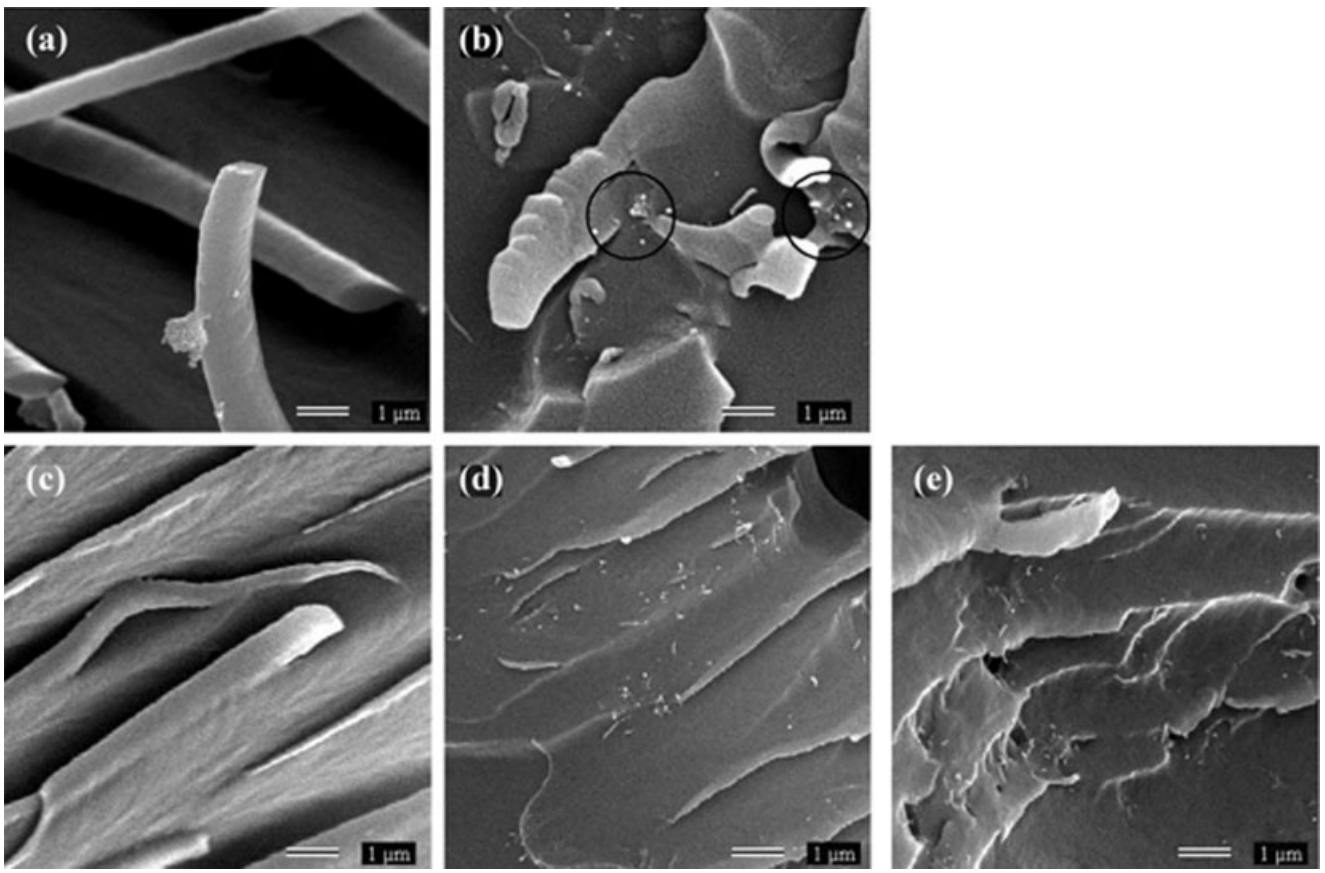

Figure 4 High-magnification SEM images of fracture surfaces of (a) the neat epoxy resin, (b) the 0.1 wt % MWNT/epoxy composite (series 1), (c) the neat epoxy resin prepared with a solvent (acetone), (d) the 0.25 wt % MWNT-D/epoxy composite (series 2), and (e) the 0.5 wt % MWNT-D/epoxy composite (series 2).

the derivative curves of both DSC and TMA curves. TMA results are discussed later. T_g values are also displayed in Table I. The DSC curves obtained for series 1 materials are very similar to the ones obtained for series 2 shown in Figure 5. The range of the glass transition is quite large, approximately 40°C for the neat epoxy. The introduction of MWNT-D did not produce a T_g variation in the case of the 0.1 wt % composite, whereas for the 0.5 wt % composite, a decoupled glass transition can be observed in the derivative curve (Fig. 5, inset). Yuen et al.[16] reported an increase of ~ 20°C in the glass transition of an MWNT/epoxy system based on a sulfone hardener. This work reported T_g's in the range of 170–190°C, and these are quite different from the values obtained for the materials in this investigation and indicate a very different amorphous structure. Furthermore, from a theoretical point of view,[20] it has been thought that the CNT species should slow down the motions of the surrounding molecules and thus increase T_g of the polymer nanocomposite; this is an assumption based on a strong interaction between the CNTs and neighboring polymer chains. However, the processing variables are as important as the formulation, and the use of a surfactant and a solvent in a dispersion stage led to a decrease in T_g in SWNT/epoxy materials in the work of Liao et al.,[9] for instance. Moreover, the

TABLE I
Electrical Conductivity, Thermal, and Thermomechanical Data for MWNT-D/Epoxy-Based Composites (Series 2)

MWNT-D (%)	Conductivity (S/m)	TG weight loss at 200°C (%)	T_g (°C)		α_1 (10^{-5} °C^{-1})	α_2 (10^{-5} °C^{-1})
			DSC	TMA		
0	5.1×10^{-12}	1	66	83	7.5	14.9
0.1	7.8×10^{-11}	1.5	68	84	7.4	14.7
0.5	2.5×10^{-7}	3	68	82	7.5	15.5

α_1 is the thermal expansion coefficient before T_g; α_2 is the thermal expansion coefficient after T_g.

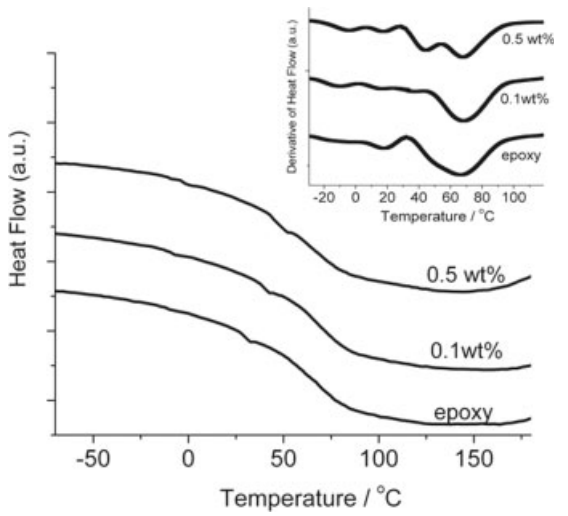

Figure 5 DSC curves of MWNT-D/epoxy composites (series 2). The inset shows the derivative of heat flow in the glass-transition region. Compositions are indicated.

recent report by Wang et al.[23] also shows a decrease in the epoxy/SWNT glass transition for both pristine and functionalized CNTs. In this work, the differences related to the main transition are in the range of T_g accuracy both for series 1 and 2. However, the presence of a second peak in the heat flow derivative of the 0.5 wt % MWNT-D composite curve at a low temperature indicates a partial increase in the segmental motion of the epoxy system for this composite in relation to that of the neat epoxy. The glass-transition decoupling observed for the 0.5 wt % composites was reproducible in two different regions of each sample of the two preparations.

Thermomechanical behavior

Figure 6 shows TMA curves for the MWNT-D/epoxy systems (series 2). At T_g, a change in the TMA curve slope associated with the change in the thermal expansion coefficient can be observed. The unexpected undulations around T_g can be attributed to stress relief and residual solvent/surfactant influence.[26] These events make the determination of T_g from TMA more difficult. However, in general, TMA T_g values are higher than DSC ones (Table I).

The thermal expansion coefficients obtained before and after T_g are similar to those of other DGEBA epoxy systems in the literature. For instance, Kim et al.[26] reported neat epoxy thermal expansion coefficients of 6.7×10^{-5} °C^{-1} before T_g and 17×10^{-5} °C^{-1} after T_g. These authors observed a decrease in the thermal expansion coefficient with the addition of organoclay to their nanocomposites. Yuen et al.[16] reported a thermal expansion coefficient close to 6×10^{-5} °C^{-1} before T_g for a neat epoxy based on a sulfone hardener and MWNT/epoxy composites. Wang et al.[23] also observed a thermal expansion coefficient close to 6.5×10^{-5} °C^{-1} before T_g for an epoxy system and values in the range of 6 to 3×10^{-5} °C^{-1} for nanocomposites based on pristine and modified SWNTs.

The thermal expansion coefficients before and after T_g of the MWNT-D composites (Table I) show a tendency of stability. A possible increase in thermal expansion was not observed. The nanotube dispersion was improved by the solvent-assisted treatment in this work, but it did not have a clear influence on the thermal expansion coefficient in the composition range studied. Looking for a possible explanation for this behavior, we should consider that the thermal expansion coefficient values of MWNT and SWNT bundles determined by X-ray diffraction studies by Maniwa et al.[18,19] indicate that the results presented here are expected. The thermal expansion coefficient of $\sim 2.6 \times 10^{-5}$ K^{-1} is probably applicable to the MWNT employed in this work, as it was produced by chemical vapor deposition and should have a defective structure. Moreover, the presence of MWNT bundles is likely, and because the thermal expansion coefficient for the MWNT intertube gap may be not much different from the value for SWNT ropes [$(4.2 \pm 1.4) \times 10^{-5}$ K^{-1}], it must be noted that this value is close to the neat epoxy resin values of the thermal expansion coefficient before T_g (Table I). Therefore, the influence of either isolated MWNT or nanotube bundles on the value of the thermal expansion coefficient before T_g (and the thermal expansion coefficient after T_g) is probably not significant. Furthermore, although the addition of nanotubes to the epoxy in the low concentration range studied (up to 0.5 wt %) showed a significant influence on conductivity levels, it did not produce simultaneous variations in the thermomechanical parameters of the thermal expansion coefficient.

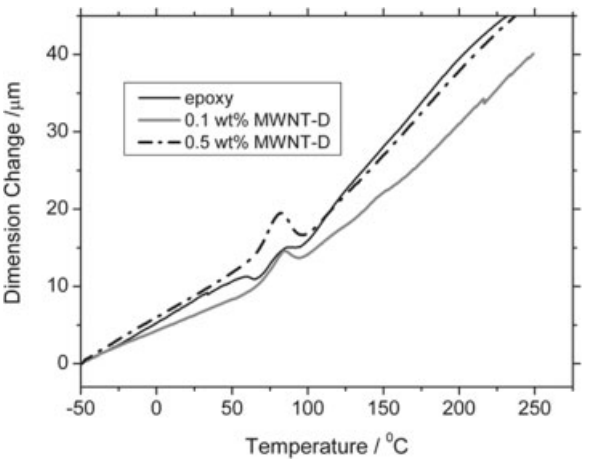

Figure 6 TMA curves (expansion mode) of MWNT-D/epoxy composites (series 2). Compositions are indicated.

CONCLUSIONS

MWNTs were debundled with surfactant/acetone in a process involving strong sonication and stirring. The nanotube bundle dispersion was significantly enhanced by the use of solvent/sonication to mix MWNT-D into the epoxy. The nanocomposite thermomechanical properties did not show changes in relation to the neat epoxy. On the other hand, the range of compositions studied, up to 0.5 wt %, showed a significant increase in the electrical conductivity. These associated behaviors may be considered an advantage in the case of polymer nanocomposites required for electrostatic dissipation, which might be processed with the same apparatus used for neat epoxy, as the volume changes will not be different. The invariability of the thermal expansion coefficients of nanocomposites is explained by the thermal expansion coefficient values previously determined for MWNT and intertube gaps[18,19] and that of the neat epoxy.

The authors are grateful for the infrared microscopy images provided by Laboratório de Inclusões Fluidas e Metalogênese (Centro de Desenvolvimento da Tecnologia Nuclear/Comissão Nacional de Energia Nuclear). The authors also thank Adelina P. Santos and Luiz O. Ladeira for fruitful discussions.

References

1. (a) Saito, R.; Dresselhaus, G.; Dresselhaus, M. S. Physical Properties of Carbon Nanotubes; Imperial College Press: London, 1998; (b) Dresselhaus, M. S.; Dresselhaus, G.; Eklund, P. C. Science of Fullerenes and Carbon Nanotubes; Academic: New York, 1996; (c) Poncharal, P.; Wang, Z. L.; Ugarte, D.; de Heer, W. A. Science 1999, 283, 1513.
2. Ajayan, P. M.; Stephan, O.; Colliex, C.; Trauth, D. Science 1994, 265, 1212.
3. Gojny, F. H.; Wichmann, M. H. G.; Kopke, U.; Fiedler, B.; Schulte, K. Compos Sci Technol 2004, 64, 2363.
4. Ajayan, P. M.; Schadler, L. S.; Giannaris, C.; Rubio, A. Adv Mater 2000, 12, 750.
5. Breton, Y.; Desarmot, G.; Salvetat, J. P.; Delpeux, S.; Sinturel, C.; Beguin, F.; Bonnamy, S. Carbon 2004, 42, 1027.
6. Valentini, L.; Puglia, D.; Frulloni, E.; Armentano, I.; Kenny, J. M.; Santucci, S. Compos Sci Technol 2004, 64, 23.
7. Sandler, J. K. W.; Kirk, J. E.; Kinloch, I. A.; Shaffer, M. S. P.; Windle, A. H. Polymer 2003, 44, 5893.
8. Wang, Z.; Liang, Z. Y.; Wang, B.; Zhang, C.; Kramer, L. Compos A 2004, 35, 1225.
9. Liao, Y.-H.; Marietta-Tondim, O.; Liang, Z.; Zhang, C.; Wang, B. Mater Sci Eng A 2004, 385, 175.
10. Lau, K.-T.; Lu, M.; Lam, C.-K.; Cheug, H.-Y.; Sheng, F.-L.; Li, H.-L. Compos Sci Technol 2005, 65, 719.
11. Zhu, J.; Peng, H.; Rodriguez-Macias, F.; Margrave, J. L.; Khabashesku, V. N.; Imam, A. M.; Lozano, K.; Barrera, E. V. Adv Funct Mater 2004, 14, 643.
12. Barrau, S.; Demont, P.; Peigney, A.; Laurent, C.; Lacabanne, C. Macromolecules 2003, 36, 5187.
13. Bryning, M. B.; Islam, M. F.; Kikkawa, J. M.; Yodh, A. G. Adv Mater 2005, 17, 1186.
14. Gojny, F. H.; Wichmann, M. H. G.; Fiedler, B.; Kinloch, I. A.; Bauhofer, W.; Windle, A. H.; Schulte, K. Polymer 2006, 47, 2036.
15. Li, N.; Huang, Y.; Feng, D.; Xiabo, H.; Xiao, L.; Gao, H.; Ma, Y.; Li, F.; Chen, Y.; Eklund, P. C. Nano Lett 2006, 6, 1141.
16. Yuen, S.-M.; Ma, C.-C. M.; Wu, H.-H.; Kuan, H.-C.; Chen, W.-J.; Liao, S.-H.; Hsu, C.-W.; Wu, H.-L. J Appl Polym Sci 2007, 103, 1272.
17. Gojny, F. H.; Wichmann, M. H. G.; Fiedler, B.; Schulte, K. Compos Sci Technol 2005, 65, 2300.
18. Maniwa, Y.; Fujiwara, R.; Kira, H.; Tou, H.; Kataura, H.; Suzuki, S.; Achiba, Y.; Nishibori, E.; Takata, M.; Sakata, M.; Fujiwara, A.; Suematsu, H. Phys Rev B 2001, 64, 241402.
19. Maniwa, Y.; Fujiwara, R.; Kira, H.; Tou, H.; Nishibori, E.; Takata, M.; Sakata, M.; Fujiwara, A.; Zhao, X.; Iijima, S.; Ando, Y. Phys Rev B 2001, 64, 073105.
20. Wei, C.; Srivastava, D.; Cho, K. Nano Lett 2002, 2, 647.
21. Guo, H.; Sreekumar, T. V.; Liu, T.; Minus, M.; Kumar, S. Polymer 2005, 46, 3001.
22. Xu, Y.; Ray, G.; Abdel-Magid, B. Compos A 2006, 37, 114.
23. Wang, S.; Liang, Z.; Gonnet, P.; Liao, Y.-H.; Wang, B.; Zhang, C. Adv Funct Mater 2007, 17, 87.
24. Delpeux, S.; Szostak, K.; Frackowiak, E.; Bonnamy, S.; Béguin, F. J Nanosci Nanotechnol 2002, 2, 481.
25. Connell, M. J. O.; Bachilo, S. M.; Huffman, C. B.; Moore, V. C.; Strano, M. S.; Haroz, E. H.; Rialon, K. L.; Boul, P. J.; Noon, W. H.; Kittrell, C.; Ma, J.; Hauge, R. H.; Weisman, R. B.; Smalley, R. E. Science 2002, 298, 593.
26. Kim, J.-K.; Hu, C.; Woo, R. S. C.; Shan, M. L. Compos Sci Technol 2005, 65, 805.